Grid Wear Analysis of a Miniature Ion Engine

IEPC-2015-187／ISTS-2015-b-187

Presented at Joint Conference of 30th International Symposium on Space Technology and Science
34th International Electric Propulsion Conference and 6th Nano-satellite Symposium,
Hyogo-Kobe, Japan
July 4 – 10, 2015

M. Nakano[1]
Tokyo Metropolitan College of Industrial Technology, Tokyo, 116-8523, Japan

H. Koizumi[2]
The University of Tokyo, Tokyo, 113-8654, Japan

Abstract: This paper focuses on the variation in extraction-ion beam performances in a miniature ion engine due to grid erosion. Because speed and cost are very important issues in microspacecraft development, we replace time-consuming grid wear tests with numerical simulations using the JAXA Ion Engine Development Initiatives (JIEDI) tool. By comparing the results obtained for a miniature ion engine with those of a μ10 ion engine, we observe differences in the variation of extraction-ion beam performance for miniature and ordinary-sized ion engines. The use of a gimballing device in a miniature-ion engine results in a significant mass penalty, and we present a numerical simulation for predicting erosion-induced variations in the thrust-vector direction in an ion engine.

Nomenclature

c	=	conductance
D	=	grid hole diameter
J	=	beam current
l_g	=	separation distance between the screen and accelerator grids
t	=	thickness
T_d	=	designed lifetime
v	=	velocity
V	=	voltage
β	=	beam deflection angle
$\bar{\beta}$	=	time-averaged beam deflection angle
ϕ	=	open area fraction
Γ	=	neutral flux
η_u	=	propellant utilization efficiency
Subscript		
a	=	accelerator grid
BOL	=	beginning of life
s	=	screen grid
x, y, z	=	x, y, z components

[1] Associate Professor, Department of Engineering, mnakano@acp.metro-cit.ac.jp.
[2] Associate Professor, Department of Aeronautics, koizumi@al.t.u-tokyo.ac.jp.

I. Introduction

Ion engines can provide substantial propellant savings compared with chemical propulsion. While the number of space missions using ion engines continues to increases, they all involve middle- or large-size spacecraft.

In recent years, there has been increased use of microspacecraft, which are expected to reduce the speed of development, cost, and flexibility of space missions. There have also been extensive efforts to realize miniature propulsion systems. Miniature ion-engine systems are therefore being applied to microspacecraft, such as the Miniature Ion Propulsion System (MIPS) and the Ion thruster and COld-gas thruster Unified Propulsion System (I-COUPS), which were developed at the University of Tokyo.[1-3]

While these are significant advancements, the miniaturization of ion engines introduces technical problems that have been resolved for ordinary-sized ion engines, namely a shorter grid lifetime caused by erosion, which is due to the low plasma-production efficiency,[4] and the absence of a gimballing device to act as a countermeasure against thrust-vector movements during flight.

Owing to its limited capacity for plasma generation, the extraction ion-beam current and the propellant utilization efficiency of miniature ion engines are lower than those of standard-sized ion engines. Therefore, small ion engines experience severe erosion and significant performance degradation because sputtering particles are generated mainly at a propellant utilization efficiency of 0.5, which is close to their operational ranges. For example, the propellant-utilization efficiencies of the above-mentioned MIPS and I-COUPS ion engines are around 0.4 because of their lower ion production. In view of the current and potential growth in the use of small ion engines, it is very important to perform a lifetime analysis that includes changes in the extraction ion-beam performance. A previous study[4] was the first to include such an effect in a complete three-dimensional analysis using the JAXA Ion Engine Development Initiative (JIEDI) tool.

The use of a gimballing device in a miniature ion-engine system results in a significant mass penalty. For example, the gimballing system of the ion engine in the Deep Space 1 mission weighed ~15 kg and its thruster head weighed 8 kg.[5] Thus, the removal of the gimballing system and the use of other torque-cancelling mechanisms such as the combination of a momentum wheel and unloading by a reaction-control system is a realistic approach, and this is employed in I-COUPS. In this case, the minimization of the torque generated by the ion engine is important. In this study, we also focus on the changes in the thrust-vector direction due to erosion. We performed parametric analyses to investigate the effect of the grid displacement and its magnitude on the change of the thrust-vector directions. To mitigate the loss of the thrust-vector movement due to erosion, we obtained the best initial thruster setting angle.

II. Modeling

In this section, we present a brief explanation of the JIEDI tool.[6,7] We then discuss the physical and numerical modeling for the nominal and off-axis analyses.

A. JIEDI Tool

The JIEDI tool was developed to qualify ion-engine optics with high precision and accuracy. Figure 1 shows the analysis region of the JIEDI tool.

Figure 2 shows a schematic diagram of the erosion mechanism of ion-acceleration grids. When ions/neutrals generated by elastic scattering (SCAT) or charge-exchange (CEX) collisions hit the grid surface, it is eroded by sputtering. While most of the eroded grid atoms flow away, some of them are re-deposited on the grid surface. As is

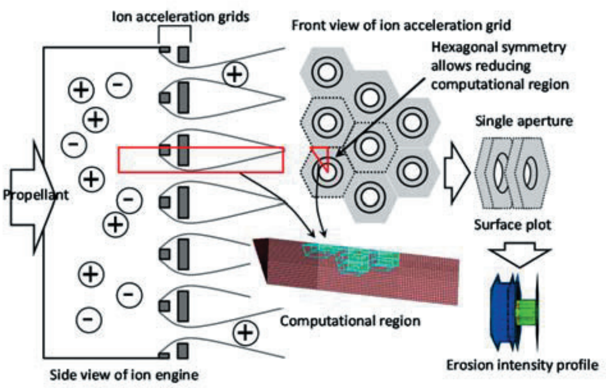

Figure 1. JIEDI tool analysis.

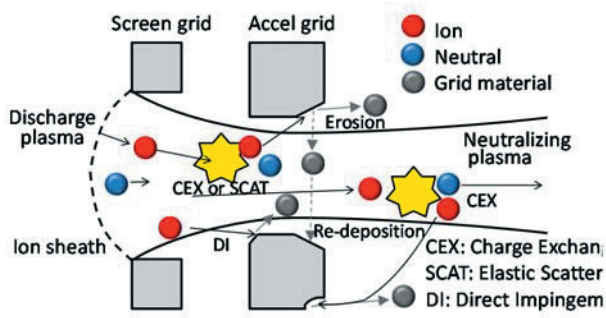

Figure 2. Grid erosion mechanism.

Table 1. Geometric and operating parameters.

Parameter	Values
D_s, D_a	0.80 mm, 0.40 mm
ϕ_s	0.67
t_s, t_a, l_g	0.20 mm, 0.30 mm, 0.30 mm
V_s, V_a	1500 V, −350 V
Ion-beam current	0.021 mA/hole
η_u	0.42
Grid material	Molybdenum

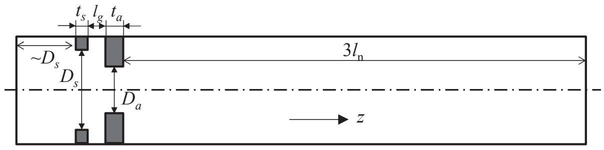

Figure 3. Computation region.

the case with many ion-optics studies,[8,9] the JIEDI tool can analyze these physical phenomena that are associated with grid erosion and re-deposition. The numerical scheme used in the JIEDI tool is a hybrid fluid-particle approach, in which ions and neutrals are treated as particles and electrons are treated as fluid. The JIEDI tool incorporates the latest sputtering models to account for the sputtered grid material's movements and its re-deposition onto the grid surface. The computational region upstream and downstream from the grids are shown in Figure 3. The upstream plasma region has a length of around D_s and the length of the downstream region is three-times that of neutralization length l_n.[10] The JIEDI tool employs the finite element method (FEM) for discretization, and its grid size was determined from a previous study.[11]

B. Nominal Condition

Table 1 lists the calculation conditions of the miniature ion engine based on MIPS and I-COUPS. The engine is a two-grid system with molybdenum grids, and it uses xenon as the propellant. The propellant flow rate was fixed during the operation and the doubly charged ion fraction was assumed to be 0.10 based on data obtained from other microwave ion engines.[12] In the numerical wear test, ion beams and neutrals were assumed to be uniform in the radial direction, and we therefore used the average values of the ion-beam current and neutral flux.

Intense grid erosion significantly changes the conductance of grids, and this lowers the neutral number density in the discharge chamber, causing ion production and ion-beam extraction to deteriorate significantly. In this study, we used a simple model where the ion-beam current is proportional to the neutral number density in the discharge chamber. In this model, the conductance was used to reflect the change in the grid shape, and the ion-beam current can be expressed as:

$$J = J_{\mathrm{BOL}} \times \left(\frac{\eta u_{\mathrm{BOL}}}{1-\eta u_{\mathrm{BOL}}} + 1\right) \Big/ \left(\frac{\eta u_{\mathrm{BOL}}}{1-\eta u_{\mathrm{BOL}}} + \frac{C}{C_{\mathrm{BOL}}}\right). \tag{1}$$

This is a decreasing function of the grid conductance. In contrast, the neutral flux is an increasing function of the conductance, which is given as:

$$\Gamma = \Gamma_{\mathrm{BOL}} \times \left(\frac{\eta u_{\mathrm{BOL}}}{1-\eta u_{\mathrm{BOL}}} + 1\right) \Big/ \left(\frac{\eta u_{\mathrm{BOL}}}{1-\eta u_{\mathrm{BOL}}} + \frac{C}{C_{\mathrm{BOL}}}\right) \times \frac{C}{C_{\mathrm{BOL}}}, \tag{2}$$

where the grid-conductance ratio is evaluated in the neutral-density calculation module of the JIEDI tool from the ratio of the number of super particles leaving the downstream boundary (located downstream of the accelerator grid) to those entering the upstream boundary (located upstream of the screen grid).

To compare the simulation results with those of standard-sized microwave ion engines, we also evaluated the change in the extraction-ion beam performance of the μ10 ion engine using the simulation results.[6]

C. Grid Offset

The calculation mesh was constructed using the displacement of ε, as shown in Figure 4. The relationship between the grid displacement and the beam deflection angle is given by linear optics theory[13]:

$$\beta = -\varepsilon/4l_g. \tag{3}$$

Eq. (3) is in good agreement near $\beta = 0$. However, it differs for large deflection angles.[14] According to Eq. (3), a rough estimate of the grid displacement is ~0.0335 mm for a beam-deflection angle of 1.6°. Using this value, we performed several calculations to accurately determine the value of the initial grid offset. In this study, the grid

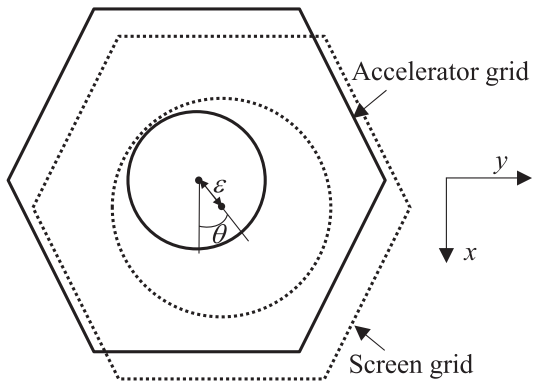

Figure 4. Definition of grid displacement and angle.

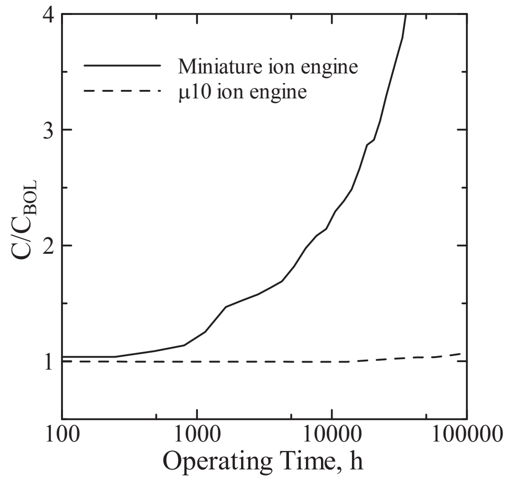

Figure 5. Comparison of variation in grid conductance ratio.

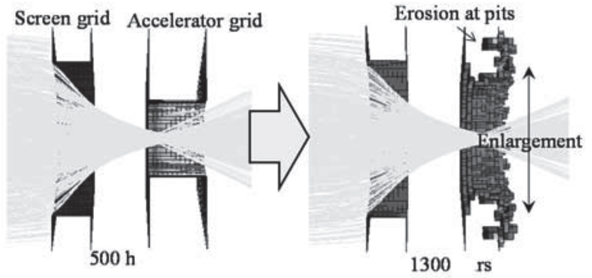

Figure 6(a). Ion beam trajectories and grid surfaces.

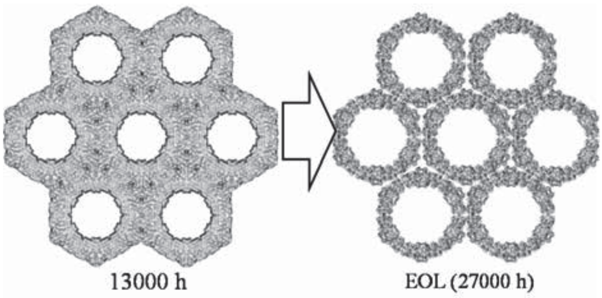

Figure 6(b). Downstream face of accelerator grid; pit-and-groove pattern erosion separates ion extraction grid holes at EOL.

displacement was set to be 0.045 mm.

To investigate the effect of the initial grid offset direction, the grid-offset angle θ is defined as shown in Figure 4, and we analyzed three cases considering the symmetry of the grid holes: (a) 0°, (b) 30°, and (c) 45°. In addition, we also studied the effect of the magnitude of the initial thrust-vector offset, while the initial displacement was changed from 0.0112 mm (0.4°) to 0.045 mm (1.6°).

In the JIEDI tool, the beam-deflection angle was calculated from the sum of the x, y, and z components of the momentum of each ion beam:

$$\beta = \tan^{-1}\left(\sqrt{(\sum Jv_x)^2 + \left(\sum Jv_y\right)^2}/\sum Jv_z\right). \tag{3}$$

The x- and y-components of the beam-deflection angle are given as

$$\beta_x = \tan^{-1}(\sum Jv_x/\sum Jv_z) \tag{4}$$

$$\beta_y = \tan^{-1}\left(\sum Jv_y/\sum Jv_z\right) \tag{5}$$

The plot of β_x and β_y shows the movement of the ion-beam center.

III. Results and Discussion

A. Nominal Condition

Figure 5 compares the changes in the grid conductance of the miniature ion engine and μ10 ion engine. As is evident from the figure, the grid conductance in the miniature ion engine increased significantly; however, it remained almost constant in the μ10 ion engine. This result highlights the importance of including the change in the extraction beam performance, especially if the erosion rate is high, as in the case of the miniature ion engine considered here.

Figure 6(a) shows the change in the ion-beam trajectories and grid surfaces after operating for 500 h and 13000 h, respectively. As seen in the figure, the ion beams are focused on the centerline near the upper surface of the accelerator grid, and they expand at large angles. As the miniature ion engine operates at an ion-beam current that is one order of magnitude smaller than that of ordinary-sized ion engines, its ion beam trajectories follow this path because ions operating at a small ion beam current tend to be accelerated at highly diverted angles.

Figure 6(b) shows the downstream surface views of the accelerator grid after operating for 13000 h and 27000 h. We observe the enlarged diameters of the accelerator grid holes and the formation of pit-and-groove patterns, which were due to erosion. Eventually, the bridges between the acceleration grid holes were completely eroded, and this resulted in a structural failure of the grid system.

Figure 7 shows the variation in the propellant-utilization efficiency as a function of the operation time. At the

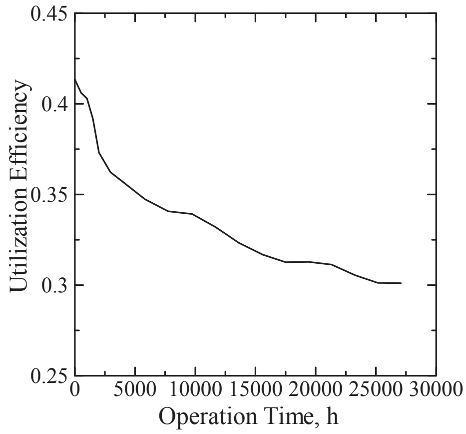

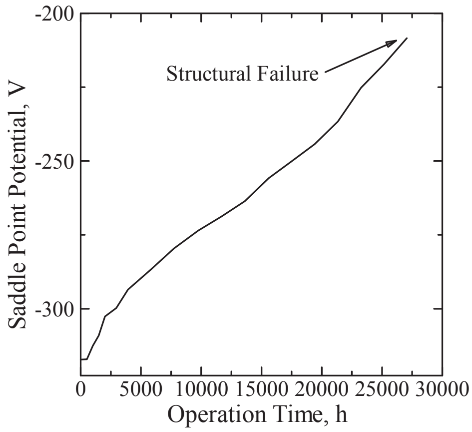

Figure 7. Propellant utilization efficiency and operation time. **Figure 8. Saddle point potential and operation time.**

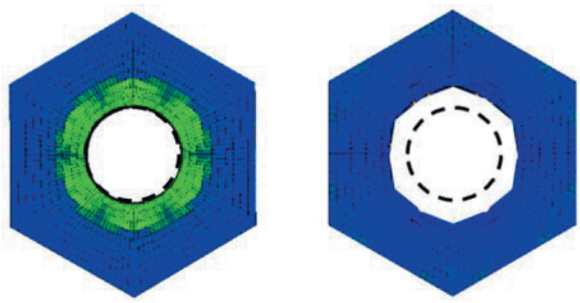

Upstream Face Downstream Face

Figure 9. Simulated accelerator grid surface after 156-h operation.

Upstream Face Downstream Face

Figure 10. Photographs of accelerator grid after 181-h operation in the central region.[15]

BOL, the value was around 0.42. For the first 2000 h, it decreased at a fast rate because of the rapid change in the diameter of the accelerator grid hole, which was caused by the direct impingement of mainstream ion beams, as well as erosion due to the high-energy CEX and SCAT ions and neutrals. After 2000 h, the value decreased at almost the same rate as CEX and SCAT erosion was the dominant effect. At the EOL, the propellant utilization efficiency decreased by around 30% compared to that at the BOL.

Figure 8 shows the variation in the saddle point potential, which must be negative to prevent neutralizing electrons from backstreaming. As seen in the figure, the value remained negative until the grid was eroded away at 27000 h, which is much longer than the typical required lifetime of 10000 h for miniature ion engines. These results indicate that miniature ion engines can withstand 10000 h of operation; however, their propulsion performance degrades substantially thereafter because of severe accelerator grid erosion.

Figures 9 and 10 compare the grid shapes after around 200 h of operation. As seen in Figure 9, the downstream face of the accelerator grid was eroded in a 6-point star shape by the direct impingement of mainstream ion beams. In contrast, the upstream face had a region with a higher erosion rate surrounding the grid hole, where CEX and SCAT ions sputtered its surface. These erosion patterns are the same as those obtained in the experiments shown in Figure 10.

B. Grid Offset

Figure 11 shows plots of the beam center for different initial grid offsets at 0 h–5000 h. For all the initial grid offset directions, the beam center moves in the initial grid offset direction. Around the accumulated operating time of 1500 h, the beam center converges toward the physical centerline of the grid hole, and then overshoots in the opposite direction.

As shown in the figure, the differences in the values for the three initial angles are very small, and the plots all follow the same trend. This result shows that the initial grid offset direction is not a dominant parameter affecting the movement of the thrust vector. Therefore, we performed calculations only for the initial grid offset direction of θ

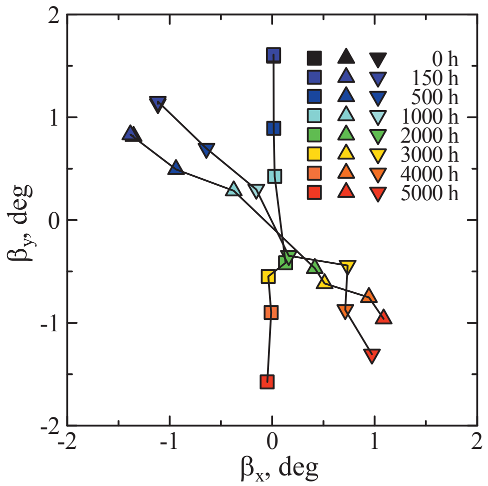

Figure 11. Plots of beam center movement.

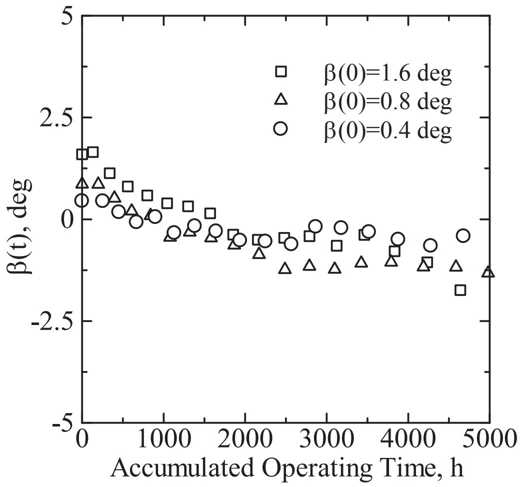

Figure 12. Beam-deflection angle and accumulated operating time.

= 0°.

Figure 12 shows plots of the beam-deflection angles $\beta(t)$ for initial grid offsets that range between 0.4° and 1.6°. In all of the initial grid offsets, the beam center moves to the physical centerline and then overshoots in the opposite direction. For a small initial grid offset of 0.4°, the movement of the beam centerline is small, and it becomes larger as the initial grid offset angle increases. This result indicates that an initial grid offset angle that is too large shortens the lifetime of the grid system, and the initial grid offset should therefore be set as small as possible.

For practical applications, the time-averaged beam-deflection angle is defined and calculated as

$$\bar{\beta}(T_d) = \int_0^{T_d} \beta(t)dt/T_d. \qquad (6)$$

Because Eq. (6) gives the averaged direction of the beam center during the designed lifetime of T_d, setting the initial thruster angle to be $-\bar{\beta}(T_d)$ can mitigate the propellant loss caused by the change in thrust-vector movement due to erosion. This results in an optimized thruster tilt angle for the designed thruster lifetime, as shown in Figure 13.

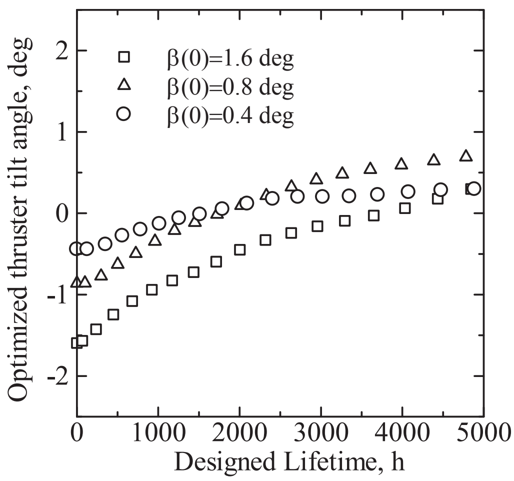

Figure 13. Optimized thruster tilt angle for designed lifetime.

IV. Conclusion

In this study, we analyzed variations in the extraction-ion beam performance caused by erosion in a miniature ion engine. In addition, we studied the effects of the grid erosion on variations in the thrust-vector direction without the gimballing operation of the ion engines. The results are as follows:

(1) The extraction-ion beam performance deteriorated significantly because of grid erosion; however, nominal grid design parameters met the typical lifetime requirement of 10000 h with a sufficient margin. The EOL of the grid system is caused by the structural failure of the accelerator grid, and this occurred after around 27000 h of operation.

(2) The direction of the thrust vector moves to the physical centerline of the grid system because of erosion. However, the thrust vector does not remain on the physical centerline, but overshoots in the opposite direction.

(3) The beam-deflection angles were averaged according to the operating time, which helped to determine the best

initial thruster direction. By minimizing the initial grid offset and using the lifetime-averaged thrust-vector direction as the initial thruster direction, we can mitigate the propellant loss induced by the movement of the thrust vector due to erosion.

References

[1]Koizumi, H., Komurasaki, K., and Arakawa, Y., "Development of the Miniature Ion Propulsion System for 50 kg Small Spacecraft," AIAA paper 2012-3949, 2012.

[2]Koizumi, H. and Kuninaka, H., "Performance of the Miniature and Low Power Microwave Discharge Ion Engine mu-1," AIAA paper 2010-6617, 2010.

[3]Inagaki, T., Kasagi Y., Kawahara H., Asakawa J., Yaginuma K., Koizumi H., Funase R., and Komurasaki K., "Measurement of the Center of a Thrust Vector of Miniature Ion Thruster in Ion thruster and Cold-gas Thruster Unified Propulsion System (I-COUPS)," JSASS-2014-4703, Proceedings of 58th Space Sciences and Technology Conference, (2014). (in Japanese)

[4]Nakano, M., Koizumi, H., Inagaki, T., and Komurasaki, K., "Numerical Study of μ1 Ion Engine Optics Using JIEDI Tool," Transactions of the Japan Society for Aeronautical and Space Sciences, Aerospace Technology Japan, 12 (2014), ists29, pp. Pb_27-Pb_32.

[5]Polk, J., Kakuda, R., Anderson, J., Brophy, J., Rawlin, V., Patterson, M., Sovey, J., and Hamley, J., "Validation of the NSTAR Ion Propulsion System on the Deep Space One Mission - Overview and Initial Results," 35th Joint Propulsion Conf. (1999) AIAA-99-2274.

[6]Nakano, M., "JIEDI Tool: Numerical Life Qualification Tool for Ion Engine Optics," Transactions of the Japan Society for Aeronautical and Space Sciences, Aerospace Technology Japan, 10 (2012), pp. Pb_85-Pb_90.

7Funaki, I., Watanabe, H., Nakano, M., Kajimura, Y., Miyasaka, T., Nakamura, Y., Kuninaka, H., and Shinohara, I., "Numerical Lifetime Evaluation of Ion Thruster's Ion Optics using the JIEDI Tool," AIAA-2012-3797, 48th AIAA/ASME/SAE/ASEE Joint Propulsion Conference & Exhibit, 2012, Atlanta.

[8]Emhoff, J. W. and Boyd, I. D., "NEXT Ion Optics Modeling of Total Thruster Performance," AIAA paper 2005-3687, 2005.

[9]Wang, J., Caoy, Y., Kafafyy, R., Martinezz, R., and Williams, J., "Ion Impingement Limits of Sub-Scale Ion Optics: Comparison of Simulation and Experiment," AIAA paper 2006-4999, 2006.

[10]Kaufman, R., "One-Dimensional Analysis of Ion Rockets," NASA TN D-261, 1960.

[11]Nakamura, Y., Yamamoto, N., Nakashima, H., and Nakano, M., "Effect of Mesh Size and Time Step on Simulation Results of Ion Acceleration Grid Erosion," Applied Plasma Science 20 (2012), pp. 33-38. (in Japanese)

[12]Nakano, M., "Doubly Charged Ion Effect on Life Prediction Accuracy of Ion Acceleration Grid System," *Vacuum*, Vol. 88 2013, pp. 70-74.

[13]Whealton, J., "Linear Optics Theory of Ion Beamlet Steering," Rev. Sci. Instrum., 48(1977), 1428.

[14]Okawa, Y., Hayakawa, Y., Miyazaki, K., and Kitamura, S., "Ion thruster thrust vectoring by ion beam deflection," JAXA-RR-04-029, (2005). (in Japanese)

[15]Inagaki, T.: "Accel Grid Erosion and its Effect by 100 hr Operation of Microwave Discharge Ion Thruster", Bachelor's Thesis, Department of Aeronautics and Astronautics, University of Tokyo, 2012.